Macromolecules

ARTICLE

pubs.acs.org/Macromolecules

Infrared Spectroscopy and X-ray Diffraction Studies of Thermal Behavior and Lamella Structures of Poly(3-hydroxybutyrate-*co*-3-hydroxyvalerate) (P(HB-*co*-HV)) with PHB-Type Crystal Structure and PHV-Type Crystal Structure

Harumi Sato,*[,†,‡] Yuriko Ando,[†,‡] Hiroshi Mitomo,[§] and Yukihiro Ozaki[†,‡]

[†]School of Science and Technology and [‡]Research Center for Environment Friendly Polymers, Kwansei-Gakuin University, Sanda 669-1337, Japan

[§]Department of Biological and Chemical Engineering, Faculty of Engineering, Gunma University, Kiryu, Gunma 376-8515, Japan

Supporting Information

ABSTRACT: Thermal behavior and lamella structures of poly(3-hydroxybutyrate-*co*-3-hydroxyvalerate), hereafter P(HB-*co*-HV) (HV = 9, 15, 21, 28.8, 58.4, 73.9, and 88.6 mol %), were investigated using infrared (IR) spectroscopy, wide-angle X-ray diffraction (WAXD), and differential scanning calorimetry (DSC). Temperature-dependent IR and WAXD measurements revealed that P(HB-*co*-HV) with low HV content (HV = 9, 15, and 21 mol %) has a PHB-type crystal structure with $CH_3\cdots O{=}C$ hydrogen bonds, whereas P(HB-*co*-HV) with high HV content (HV = 73.9 and 88.6 mol %) has a PHV-type crystal structure with $CH_2\cdots O{=}C$ hydrogen bonds. The results of IR measurements showed that the strength of the $CH_3\cdots O{=}C$ hydrogen bonds in the P(HB-*co*-HV) (HV = 9, 15, and 21 mol %) copolymers is almost the same as that in PHB, whereas in the P(HB-*co*-HV) (HV = 28.8 mol %) copolymer, the hydrogen bonds become weaker. In the case of P(HB-*co*-HV) with higher HV content (HV = 73.9 and 88.6 mol %), the effect of lamella packing on $CH_2\cdots O{=}C$ hydrogen bonding in the PHV crystal is not considerable because the side chain of the HB unit is shorter than that of the HV unit. Additionally, it seems that in the crystal structure of P(HB-*co*-HV) (HV = 58.4 mol %) there are only very weak intermolecular interactions between a C=O group and either a CH_2 group or a CH_3 group because the region of transition of the crystal structure of P(HB-*co*-HV) from the PHB type to the PHV type occurs at around 50 mol % HV content. Therefore, it is very much possible that with increasing temperature the crystal structure of P(HB-*co*-HV) (HV = 58.4 mol %) is more likely to collapse than other P(HB-*co*-HV) copolymers.

INTRODUCTION

Poly(hydroxyalkanoate)s (PHAs) have been attracting considerable interest for their use as biosynthesized polymers, and their applications to functional materials have been extensively studied.[1−10] Poly(3-hydroxybutyrate) (PHB), one of the most popular PHAs, is highly crystalline and hence is too rigid and brittle for practical applications. In order to reduce the crystallinity and increase the flexibility of PHB, comonomers with longer side chains, such as 3-hydroxyvarelate (3-HV) or 3-hydroxyhexanoate (3-HHx), are copolymerized with the 3-hydroxybutyrate (3-HB) units.[11,12]

The poly(3-hydroxybutyrate) (PHB)-based copolymers such as P(HB-*co*-HV) were commercialized by ICI Ltd. in 1985. Doi et al. reported that P(HB-*co*-HV) with a wide range of 3HV contents from 0 to 95 mol % are produced in *A. eutrophus* using pentanoic and butyric acids as carbon sources.[13] Figure 1 compares the chemical structures of PHB, PHV, and P(HB-*co*-HV). It is known that P(HB-*co*-HV) shows an isomorphic crystal structure.[11,14−19] The isomorphism and transformation of the crystal structure of P(HB-*co*-HV) have been studied extensively in the past using differential scanning calorimetry (DSC), wide-angle X-ray diffraction (WAXD), solid-state NMR spectroscopy, and polarized microscopy.[11,14−19]

The crystal structure of P(HB-*co*-HV) copolymer changes from a PHB lattice to a PHV lattice at ca. 50 mol % HV.[14,19] In the case of P(HB-*co*-HV) copolymers with low HV content, the HV units intercalate in the PHB crystal structure, whereas the HB units intercalate in the PHV crystal structure in samples with high HV content. The melting temperature, T_m, and crystallinity, χ_c, of the P(HB-*co*-HV) copolymers have their minimum values at around 40−60 mol % HV content. For example, the melting temperature and crystallinity of PHV are T_m = 118 °C and χ_c = 70%, respectively, while those of P(HB-*co*-HV) (HV = 40 mol %) are T_m = 70 °C and χ_c = 40%. In 1995, Mitomo et al. found that the PHB and PHV types of crystal are found in the range of 36−56 mol % of HV content.[19] Yamada et al. reported a narrower region in 2001.[17] However, there have been few studies on the intermolecular interactions in P(HB-*co*-HV) copolymers with high HV content.

In our previous studies, we reported that there is a particular inter- or intramolecular interaction between the C=O group and the CH_3 group in PHB along the *a* axis.[20−24] On the other hand, it was found that PHV has $C{-}H\cdots O{=}C$ hydrogen bonds

Received: July 12, 2010
Revised: February 22, 2011
Published: March 16, 2011

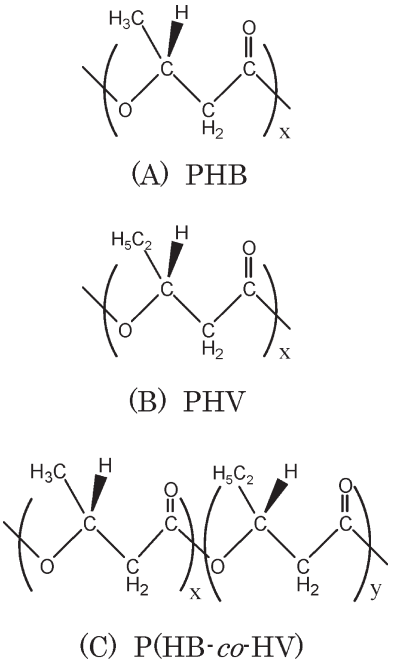

Figure 1. Chemical structures of (A) poly(3-hydroxybutyrate) (PHB), (B) poly(3-hydroxybutyrate-*co*-3-hydroxyvarelate) (P(HB-*co*-HV)), and (C) poly(3-hydroxyvarelate) (PHV).

between the C═O group and the CH_2 groups in both the main chain and side chain.[20] The peculiar chain folding of PHB lies in the (110) to (1$\bar{1}$0) (*a* axis) direction.[9,27] However, the chain folding direction of PHV is given to the (110) direction of the crystal structure.[20,25,26] The direction is the same as that of the C−H···O═C hydrogen bonds between the C═O group and the CH_2 group. The differences in the chain folding directions between PHB and PHV may come from the differences in the inter- or intramolecular interactions in their crystal structures.[20]

The purpose of the present study is to investigate the crystal structures, hydrogen bonds, and thermal behavior of P(HB-*co*-HV) with a wide range of HV content (HV = 9, 15, 21, 28.8, 58.4, 73.9, and 88.6 mol %) at the functional group level by means of IR spectroscopy, WAXD, and DSC. We place particular emphasis in our research on the following points: (1) the extent of CH···O═C hydrogen bonding in the P(HB-*co*-HV) copolymers, (2) changes in the type and strength of hydrogen bonds with increasing HV content, and (3) the thermal behavior of these copolymers.

EXPERIMENTAL SECTION

Samples. Bacterially synthesized P(HB-*co*-HV) (HV = 9, 15, 21 mol %) were obtained from Aldrich Japan Co. Other copolymers of P(HB-*co*-HV) were synthesized and purified using previously reported methods.[14,19] Films of P(HB-*co*-HV) (HV = 9, 15, 21, 28.8, 58.4, 73.9, and 88.6 mol %) copolymers were prepared by casting their 0.5% (w/v) chloroform solutions on CaF_2 windows. The films were kept in a vacuum-dried oven at 60 °C for 12 h and were allowed to cool to room temperature.

Wide-Angle X-ray Diffraction (WAXD). The WAXD data were measured for the solvent-cast samples of P(HB-*co*-HV) in the scattering angle range of 2θ = 11.5°−18.5° by using a Rigaku RINT2100 X-ray diffractometer equipped with a scintillation detector. Radiation of wavelength 1.5418 Å (Cu Kα) was employed at generator power of 50 kV and 40 mA. The temperature dependence of the WAXD measurement was controlled using a Rigaku PT30 with an accuracy of ±0.2 °C. The films were melted above their melting temperatures T_m. Next, they were placed in a vacuum-dried oven at 60 °C for 4 h and were then allowed to cool to room temperature. Before each WAXD measurement, the cell was maintained at that temperature for 5 min to equilibrate the sample.

Table 1. Melting Temperature T_m and Crystallization Temperature T_c of PHB, P(HB-*co*-HV), and PHV

		T_m/°C	T_c/°C
PHB		164	105
		173	
P(HB-*co*-HV)	HV = 9 mol %	153	89
		169	
	HV = 15 mol %	151	102
		161	
	HV = 21 mol %	159	125
	HV = 28.8 mol %	100	71
	HV = 58.4 mol %	75	n.d.
		86	
	HV = 73.9 mol %	85	n.d.
	HV = 88.6 mol %	92	39
PHV		118	n.d.

IR Measurements. The transmission IR spectra were measured at a 2 cm^{-1} resolution using a Thermo Nicolet NEXUS 470 Fourier transform IR spectrometer with a liquid-nitrogen-cooled mercury−cadmium−telluride detector. A total of 512 scans were coadded for each IR spectral measurement to ensure a high signal-to-noise ratio. The temperature of the IR cell was controlled by a thermoelectric device (CN4400, OMEGA) with an accuracy of ±0.1 °C. The temperature was increased at a rate of ∼2 °C/min.

Differential Scanning Calorimetry (DSC). Differential scanning calorimetry (DSC) measurements of P(HB-*co*-HV) copolymers were performed with a Perkin-Elmer Pyris6 DSC under a nitrogen purge over a temperature range of −50 to 130 °C at heating and cooling rates of 2 and 10 °C/min, respectively. High-purity indium and zinc were used for temperature calibration, and an indium standard was used for calibration of the heat of fusion (ΔH).

RESULTS AND DISCUSSION

1. Differential Scanning Calorimetry (DSC). The melting temperature and crystallization temperature of PHV, PHB, and P(HB-*co*-HV) are summarized in Table 1. The melting point of the copolymers was measured by DSC. In the PHB-rich copolymers (HV = 9, 15, 21, and 28.8 mol %), the melting temperature decreases with increasing HV content. Contrarily, in the case of PHV-rich copolymers (HV = 58.4, 73.9, and 88.6 mol %), the melting temperature increases with increasing HV content and approaches the melting temperature of PHV homopolymer. Figure S2 depicts the results of melting temperature and heat of fusion of PHB, P(HB-*co*-HV), and PHV versus HV content. Of particular note in Table 1 and Figure S2 is that the melting temperature has its minimum value at around 50 mol % HV in the P(HB-*co*-HV) copolymers. It is well-known that P(HB-*co*-HV) copolymers have an isomorphic crystal structure where the HV (or HB) units are embedded in the HB (or HV) crystalline lattice.[11,14−19] When the P(HB-*co*-HV) copolymers have low HV content, they have a PHB-type crystal structure; because of the large steric hindrance of side chains with HV units, the

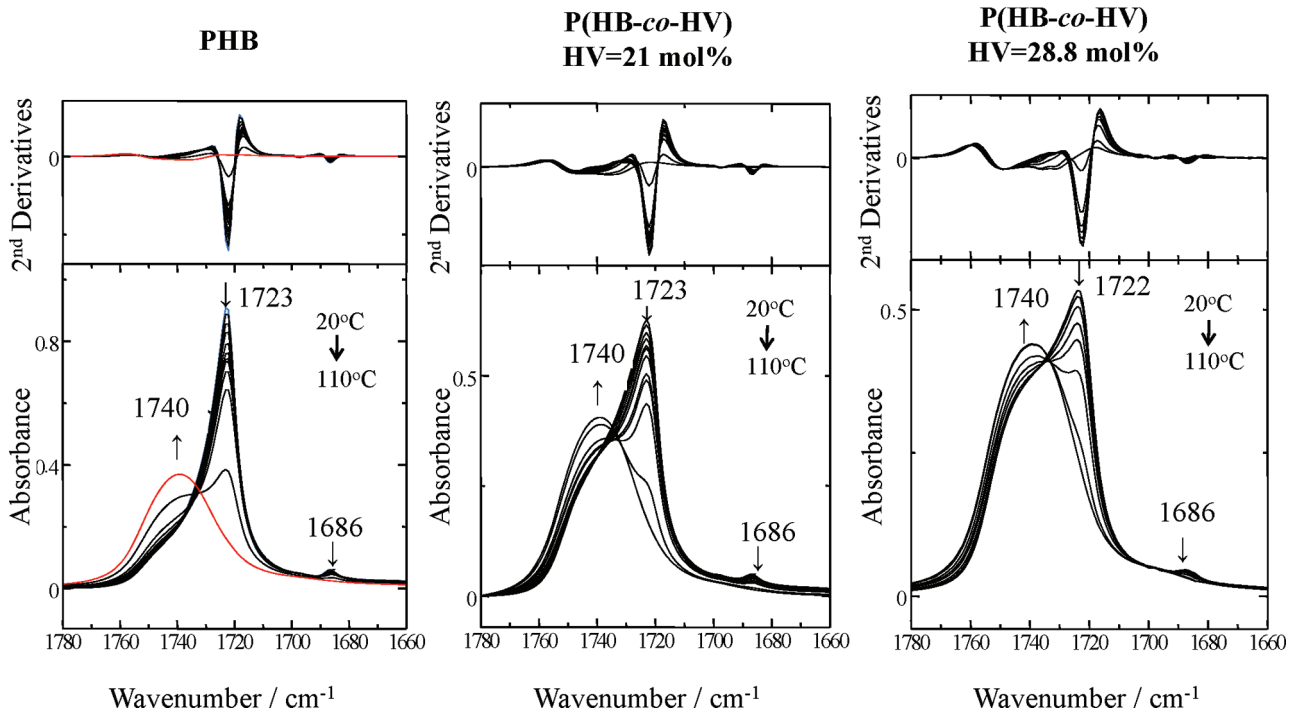

Figure 2. Temperature-dependent spectra in the C═O stretching band region (1780−1660 cm^{-1}) of (a) PHB, (b) P(HB-*co*-HV) (HV = 21 mol %), and (c) P(HB-*co*-HV)(HV = 28.8 mol %) during heating.

melting temperature and crystallinity of P(HB-*co*-HV) copolymers become lower than those of a PHB homopolymer.[11] On the other hand, when the P(HB-*co*-HV) copolymers have high HV content, they exhibit a PHV-type crystal structure.

2. C═O Stretching Band Region of IR Spectra. *2.1. PHB-Rich Copolymers (HV = 9, 15, 21, and 28.8 mol %).* Figure 2 shows temperature-dependent IR spectra in the C═O stretching band region of films of PHB and P(HB-*co*-HV) (HV = 21 and 28.8 mol %). Their second derivatives are also shown at the top of each figure. A band at 1723 cm^{-1} becomes weaker with increasing temperature while a broad feature near 1740 cm^{-1} becomes more prominent. These bands are assigned to the C═O stretching modes of crystalline and amorphous parts, respectively.[20−24] The temperature-dependent IR spectra of PHB-rich copolymers are very similar to those of PHB homopolymer not only in the C═O stretching band region but also in the C−H stretching band region (see Figure 6). The C═O stretching band appears strongly at 1723 cm^{-1} and the C−H stretching band is located above 3000 cm^{-1}, an unusually high wavenumber characteristic for the C−H···O═C hydrogen bond. Therefore, it can be concluded that a CH_3···O═C hydrogen bond exists in the P(HB-*co*-HV) crystal structure as in the case of PHB when HV content is low. In the case of P(HB-*co*-HV) (HV = 28.8 mol %), however, the intensity of the amorphous band at 1740 cm^{-1} is significantly higher than those of PHB and P(HB-*co*-HV) (HV = 9, 15, and 21 mol %). Therefore, the crystallinity of P(HB-*co*-HV) copolymers decreases with HV content as observed in Figure S2. It decreases markedly upon going from P(HB-*co*-HV) (HV = 21 mol %) to P(HB-*co*-HV) (HV = 28.8 mol %). Thermally induced alteration in the crystalline state of PHB and P(HB-*co*-HV) copolymers can be monitored by examining the temperature-dependent intensity variation of the C═O stretching band at 1723 cm^{-1}.

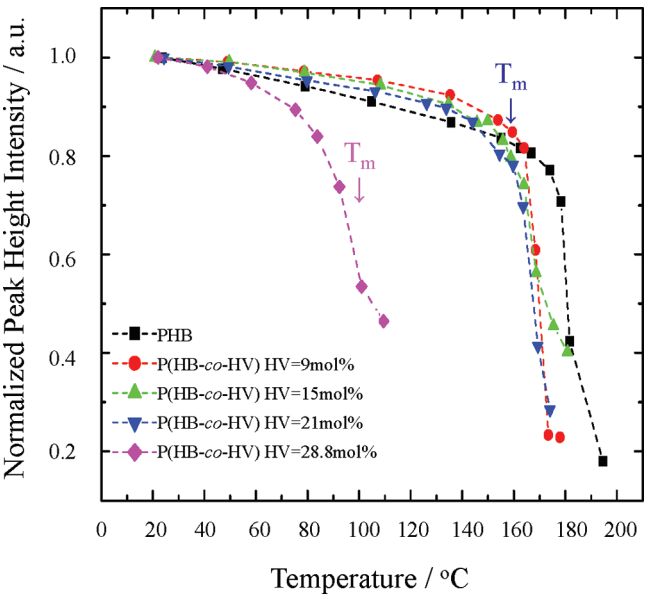

Figure 3. Plots of the normalized peak height of C═O stretching band at 1723 cm^{-1} versus temperature for PHB and P(HB-*co*-HV) (HV = 9, 15, 21, and 28.8 mol %).

Figure 3 shows a plot of the normalized peak height of the band at 1723 cm^{-1} against temperature for PHB and P(HB-*co*-HV) (HV = 9, 15, 21, and 28.8 mol %). It can be seen from Figure 3 that the intensity of the crystalline band at 1723 cm^{-1} of PHB and P(HB-*co*-HV) (HV = 9, 15, and 21 mol %) decreases only slightly from 20 to 160 °C and suddenly drops at temperatures above 170 °C, while that of P(HB-*co*-HV) (HV = 28.8 mol %) begins decreasing rapidly from fairly low temperatures compared

dx.doi.org/10.1021/ma102723n |*Macromolecules* 2011, 44, 2829–2837

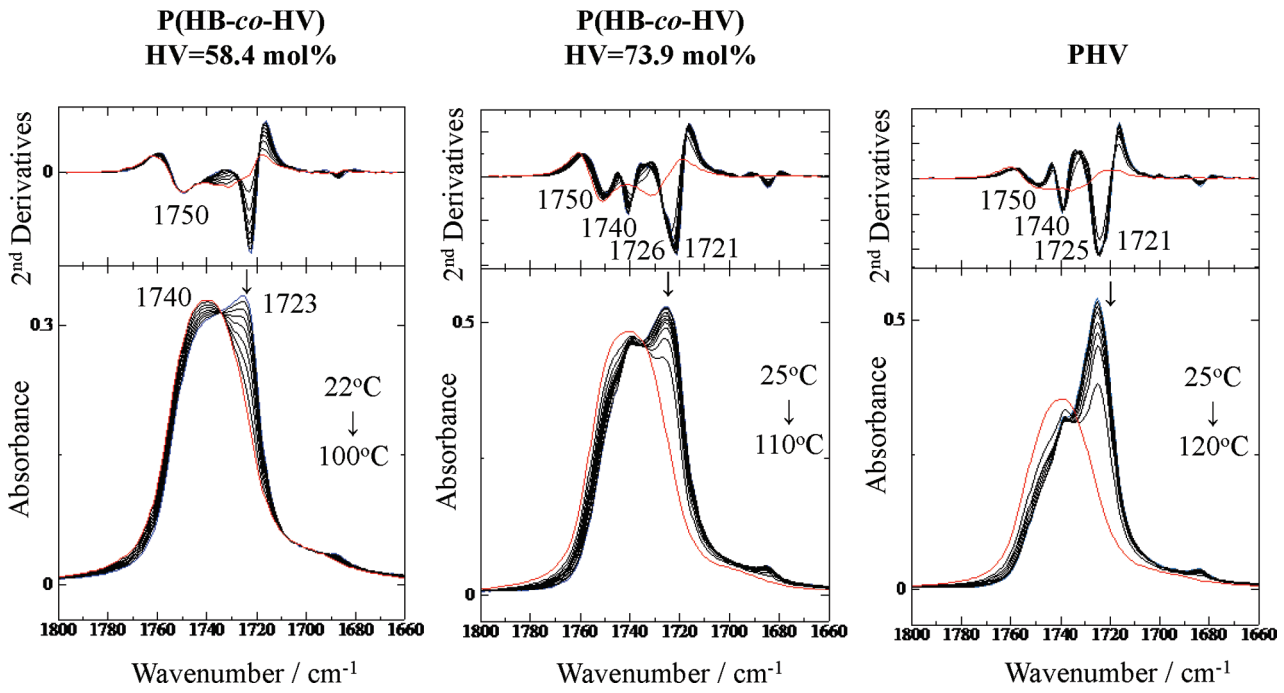

Figure 4. Temperature-dependent spectra in the C═O stretching band region of (a) P(HB-*co*-HV) (HV = 58.4 mol %), (b) P(HB-*co*-HV) (HV = 73.9 mol %), and (c) PHV during heating.

to the other copolymers. The intensity changes of the band at 1723 cm^{-1} of P(HB-*co*-HV) (HV = 9, 15, and 21 mol %) are very similar to those of the PHB homopolymer.[20−24] This similarity in the thermal behaviors of these copolymers may be understood by considering their crystal structures. Many disordered structures can exist in the crystal structure of P(HB-*co*-HV) (HV = 28.8 mol %) because of its high HV content (i.e., long side chains).

2.2. PHV-Rich Copolymers of P(HB-co-HV) (HV = 58.4, 73.9, and 88.6 mol %). Figure 4 shows temperature-dependent IR spectra (and their second derivatives) in the C═O stretching band region for films of P(HB-*co*-HV) (HV = 58.4 and 73.9 mol %) and PHV homopolymer during heating. We investigated IR spectra of PHV and assigned the bands at 1726 and 1721 cm^{-1} to the C═O group that has hydrogen bonds with both side-chain and main-chain CH_2 groups and that has a hydrogen bond with one of the CH_2 groups.[20] The 1721 cm^{-1} band was seen more clearly in the second derivative of the spectra (Figure 4). The band intensity at 1723 cm^{-1} of P(HB-*co*-HV) (HV = 58.4 mol %) and the doublet intensity near 1723 cm^{-1} of P(HB-*co*-HV) (HV = 73.9 mol %) and PHV decrease with increasing temperature. We have previously reported that the large low-frequency shift of the crystalline C═O stretching band compared to the C═O stretching band of an ester compound without hydrogen bonding (~1740 cm^{-1}) arises from the formation of a C−H···O═C hydrogen bond.[20−24] The band feature near 1723 cm^{-1} of P(HB-*co*-HV) (HV = 73.9 mol %) is similar to that of PHV (Figure 4); both have a doublet at 1726 and 1721 cm^{-1}. Thus, it is very likely that P(HB-*co*-HV) (HV = 73.9 mol %) has C−H···O═C hydrogen bonding between the CH_2 group and the C═O groups (as in the case of PHV). However, the C−H···O═C hydrogen bonding of P(HB-*co*-HV) (HV = 58.4 mol %) may be very weak as neither a CH_3 band (arising from a C−H (CH_3)···O═C hydrogen bond near 3009 cm^{-1}) nor a CH_2 bending band (due to a C−H (CH_2)···O═C hydrogen bond in the 1490−1430 cm^{-1} region) was clearly observed as will be shown later (Figures 8 and 9). It is also rather difficult to determine whether P(HB-*co*-HV) (HV = 58.4 mol %) exhibits C−H (CH_3)···O═C or C−H (CH_2)···O═C hydrogen bonding. P(HB-*co*-HV) (HV = 58.4 mol %) shows the transition of the composition of the crystal lattice from the PHB to PHV type.

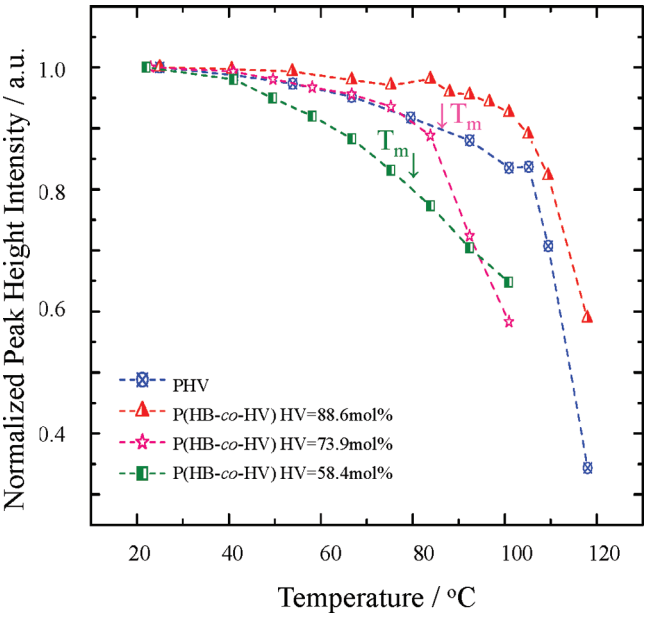

Figure 5. Plots of the normalized peak height of the C═O stretching band versus temperature for PHV and P(HB-*co*-HV) (HV = 58.4, 73.9, and 88.3 mol %).

Figure 5 shows the temperature dependence of the normalized peak height of the C═O stretching band at 1723 cm^{-1} for P(HB-

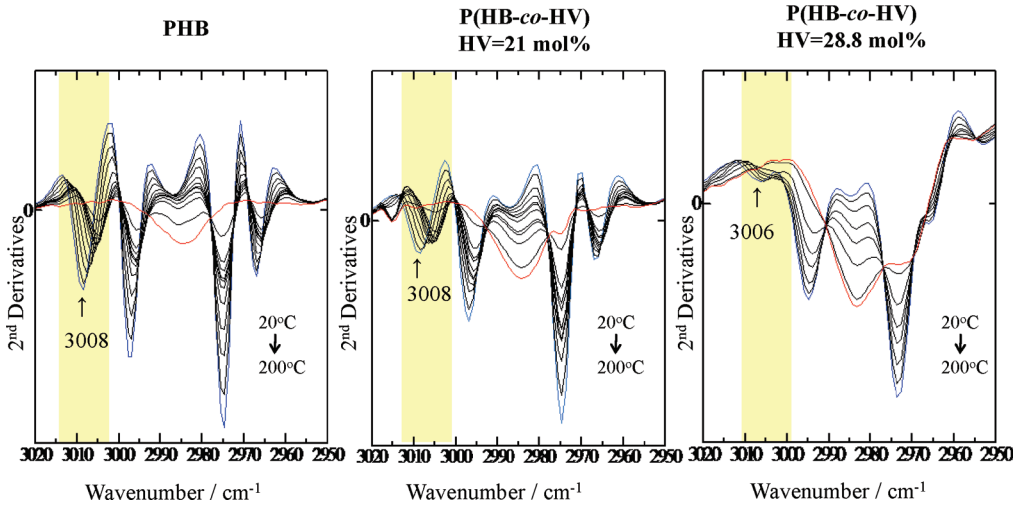

Figure 6. Temperature-dependent variations of the second derivatives in the C−H stretching band region of PHB, P(HB-*co*-HV) (HV = 21 mol %), and P(HB-*co*-HV) (HV = 28.8 mol %).

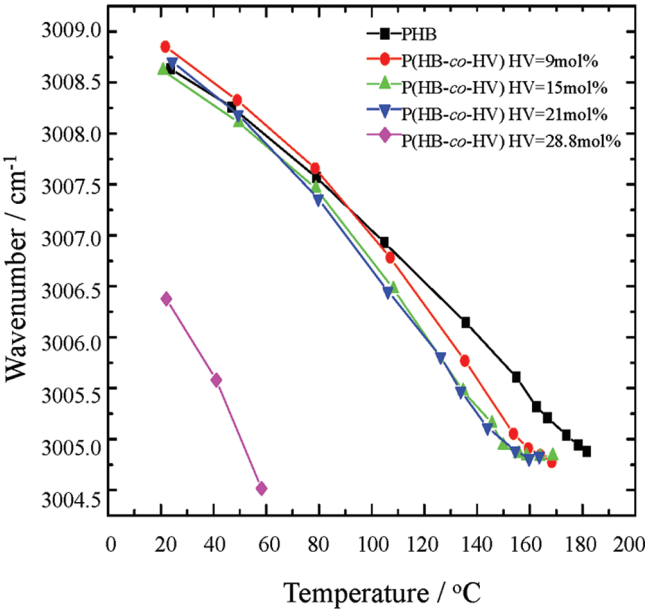

Figure 7. Plots of the wavenumber shift of the band at 3008 cm^{-1} versus temperature for PHB and P(HB-*co*-HV) (HV = 9, 15, 21, and 28.8 mol %).

co-HV) (HV = 58.4 mol %) and those at 1726 cm^{-1} for P(HB-*co*-HV) (HV = 73.9 and 88.3 mol %) and PHV. It is noteworthy that the intensity of the C═O stretching bands of PHV and P(HB-*co*-HV) (HV = 88.3 mol %) changes little until just below their melting points. The thermal behavior of this band of P(HB-*co*-HV) (HV = 88.3 mol %) is very similar to that of PHV. In the case of P(HB-*co*-HV) (HV = 58.4 mol %), however, the intensity gradually decreases from just above room temperature. This suggests that the lamella structure of P(HB-*co*-HV) (HV = 58.4 mol %) deforms easily at lower temperatures. This result is in good agreement with the result of the DSC analysis, which shows deformation of the crystal structure (thermal transition) from ~40 °C.

3. C−H Stretching Band Region of IR Spectra. *3.1. PHB-Rich Copolymers (HV = 9, 15, 21, and 28.8 mol %).* Figure 6 shows the temperature-dependent variation of the second derivatives of the C−H stretching band region of PHB and P(HB-*co*-HV) (HV = 21 and 28.8 mol %) (see original spectra of PHB and P(HB-*co*-HV) (HV = 21 and 28.8 mol %) in the 3050−2800 cm^{-1} in the Supporting Information (Figure S3)). A band at 3008 cm^{-1} is assigned to the C−H stretching mode of the CH_3 groups involved in the $CH_3\cdots O{=}C$ hydrogen bonds.[20−24] It can be seen from Figure 6 that this band appears clearly in the spectra of PHB and P(HB-*co*-HV) (HV = 21 mol %), whereas it appears only weakly in that of P(HB-*co*-HV) (HV = 28.8 mol %). Therefore, it may be concluded that the P(HB-*co*-HV) (HV = 28.8 mol %) crystal structure has fewer $CH_3\cdots O{=}C$ hydrogen bonds and, thus, collapses more easily.

Figure 7 shows a plot of the wavenumber of the C−H stretching band at 3009 cm^{-1} for PHB and P(HB-*co*-HV) (HV = 9, 15, 21, and 28.8 mol %) versus temperature during heating. It can be seen from Figure 7 that between PHB and P(HB-*co*-HV) (HV = 9, 15, 21, and 28.8 mol %) P(HB-*co*-HV) (HV = 28.8 mol %) has the C−H stretching band at a significantly lower frequency (3006 cm^{-1}), whereas the other copolymers show the C−H stretching band almost at the same frequency as that of the PHB homopolymer.[20−24] These results suggest that the strength of the $CH_3\cdots O{=}C$ hydrogen bonds of P(HB-*co*-HV) (HV = 9, 15, and 21 mol %) is almost the same as that of PHB; however, P(HB-*co*-HV) (HV = 28.8 mol %) has weaker $CH\cdots O{=}C$ hydrogen bonds. Therefore, it is very likely that the hydrogen bonds in P(HB-*co*-HV) (HV = 28.8 mol %) are weaker. These results are in good agreement with the temperature-dependent intensity change of the C═O stretching band at 1723 cm^{-1} (Figure 3).

The slopes of the plots in Figure 7 indicate the rate of weakening of the hydrogen bonds. Figure 7 shows that the slopes of P(HB-*co*-HV) (HV = 9, 15, 21 mol %) are significantly larger than that of PHB and that P(HB-*co*-HV) (HV = 28.8 mol %) has a steeper slope. Thus, it is very likely that the number of distorted and disordered structures in the P(HB-*co*-HV) copolymers increases with an increase in HV content. This result reveals that the rate of weakening of the hydrogen bonds of P(HB-*co*-HV) copolymers depends on HV content. These rates for

dx.doi.org/10.1021/ma102723n |*Macromolecules* 2011, 44, 2829–2837

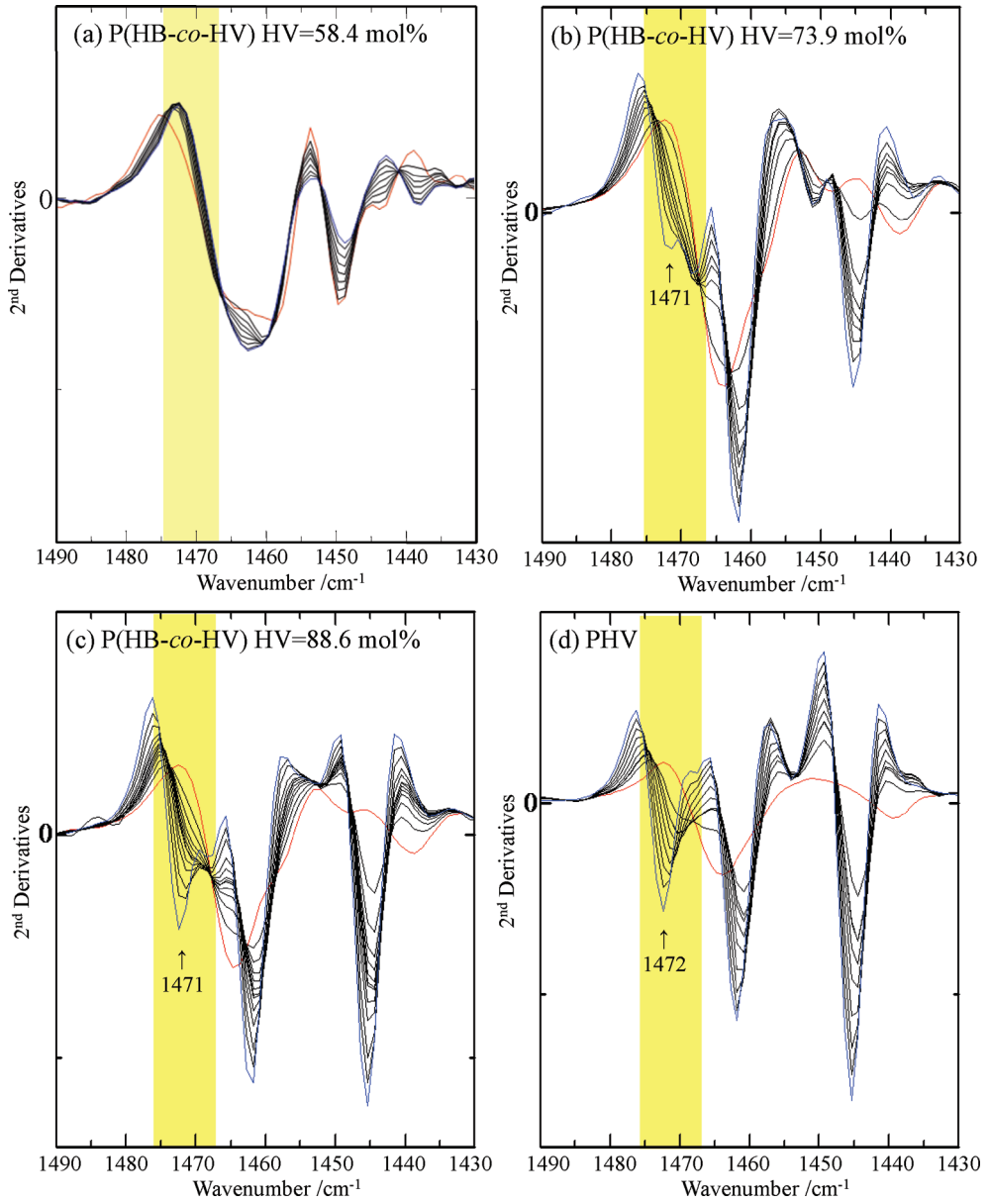

Figure 8. Temperature-dependent second-derivative spectra of P(HB-*co*-HV) (HV = 73.9 and 88.6 mol %) and PHV in the 1490−1430 cm^{-1} region.

P(HB-*co*-HV) are larger than those for PHB; particularly P(HB-*co*-HV) (HV = 28.8 mol %) shows a very rapid rate.[21−24]

3.2. PHV-Rich Copolymers of P(HB-co-HV) (HV = 58.4, 73.9, and 88.6 mol %). Figure 8 shows the second derivatives of the spectra in the 1490−1430 cm^{-1} region for films of P(HB-*co*-HV) (HV = 58.4, 73.9, 88.6 mol %) and PHV homopolymer measured during heating (see temperature-dependent spectral variations in the 1490−1420 cm^{-1} region of PHB, P(HB-*co*-HV) (HV = 28.8 mol %), and PHV in Supporting Information (Figure S4)). P(HB-*co*-HV) (HV = 73.9 and 88.6 mol %) yield a band at 1472 cm^{-1} due to CH_2 deformation of the main chain.[20] This band shows a shift by 3 cm^{-1} with a change in temperature. This observation supports the existence of C−H···O═C hydrogen bonding between the H atom of the CH_2 group in the main chain and the O atom of the C═O group in the PHV crystalline part of P(HB-*co*-HV) (HV = 73.9 and 88.6 mol %), just as in the PHV homopolymer.[20] It should be noted that in P(HB-*co*-HV) (HV = 73.9 mol %) the band at 1472 cm^{-1}, attributed to hydrogen bonding, deforms easily with temperature. It seems that the C−H···O═C hydrogen bonding between the main chain CH_2 group and the C═O group in P(HB-*co*-HV) (HV = 73.9 mol %) is weaker than that of PHV. The C−H···O═C hydrogen bonds between the CH_2 group and the C═O group seem very sensitive to crystalline packing because one of the CH_2 groups inhabits the main chain. Moreover, in P(HB-*co*-HV) (HV = 58.4 mol %), the band at 1472 cm^{-1} cannot be seen even at room temperature. Therefore, P(HB-*co*-HV) (HV = 58.4 mol %) has little hydrogen bonding between the main chain CH_2 group and the C═O group.

Figure 9 shows a plot of the shift in the band at 1472 cm^{-1} against temperature for PHV and P(HB-*co*-HV) (HV = 73.9 and 88.6 mol %) (P(HB-*co*-HV) (HV = 73.9 mol %) shows the 1472 cm^{-1} band only at room temperature). The frequencies of

dx.doi.org/10.1021/ma102723n |*Macromolecules* 2011, 44, 2829–2837

these copolymers are slightly lower than that of PHV, suggesting that the strength of the C−H···O═C hydrogen bonding of P(HB-*co*-HV) (HV = 73.9 and 88.6 mol %) is weaker than that of PHV.

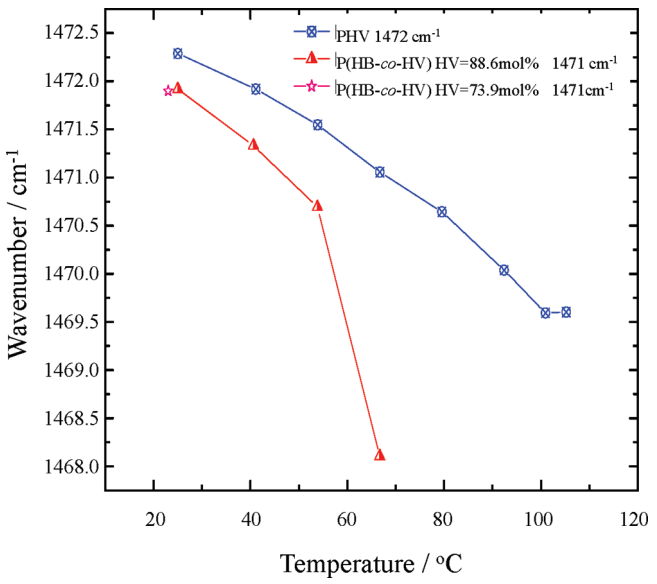

Figure 9. Plots of the wavenumber shift of the band at 1472 cm^{-1} versus temperature for PHV and P(HB-*co*-HV) (HV = 73.9 and 88.6 mol %).

4. Wide-Angle X-ray Diffraction (WAXD). Figure 10 shows the room temperature X-ray diffraction profiles of PHB and P(HB-*co*-HV) (HV = 9, 15, 21, and 28.8 mol %) and (in the right column) PHV, P(HB-*co*-HV) (HV = 58.4, 73.9, and 88.6 mol %), and PHB. P(HB-*co*-HV) (HV = 9, 15, 21, and 28.8 mol %) all form with PHB-type crystal structures.[11] All the copolymers investigated show the (020) and (110) diffraction peaks, as in the case of PHB. The lattice parameters *a* and *b*, estimated from Figure 10, of PHB and P(HB-*co*-HV) (HV = 9, 15, 21, and 28.8 mol %) are summarized in Table 2. The lattice parameter *a* of P(HB-*co*-HV) copolymers is larger than that of PHB. Because the CH_3···O═C hydrogen bonds exist along the *a* axis, the *a* spacing expands with increasing HV content, which has a longer side chain than that of an HB unit. P(HB-*co*-HV) (HV = 28.8 mol %) shows slightly larger lattice parameters *a* and *b* than the other P(HB-*co*-HV) copolymers. It seems that the order structure changes gradually throughout the whole composition range because of the large effect of steric hindrance on the long side chains of the HV unit. With an increase in HV content the crystal lattice becomes wider, and the strength of the CH_3···O═C hydrogen bond becomes weaker because of the isomorphic crystal structure. On the other hand, P(HB-*co*-HHx) (HHx = 0−12 mol %) shows almost the same value of the lattice parameter *a* because the HHx components are excluded from the lamellae. The thermal behavior of the area of the (020) diffraction peak of PHB and P(HB-*co*-HV) (HV = 9, 15, and 21 mol %) is very similar to that of the crystalline band at 1723 cm^{-1} in the C═O stretching region (Figure 5). These P(HB-*co*-HV)

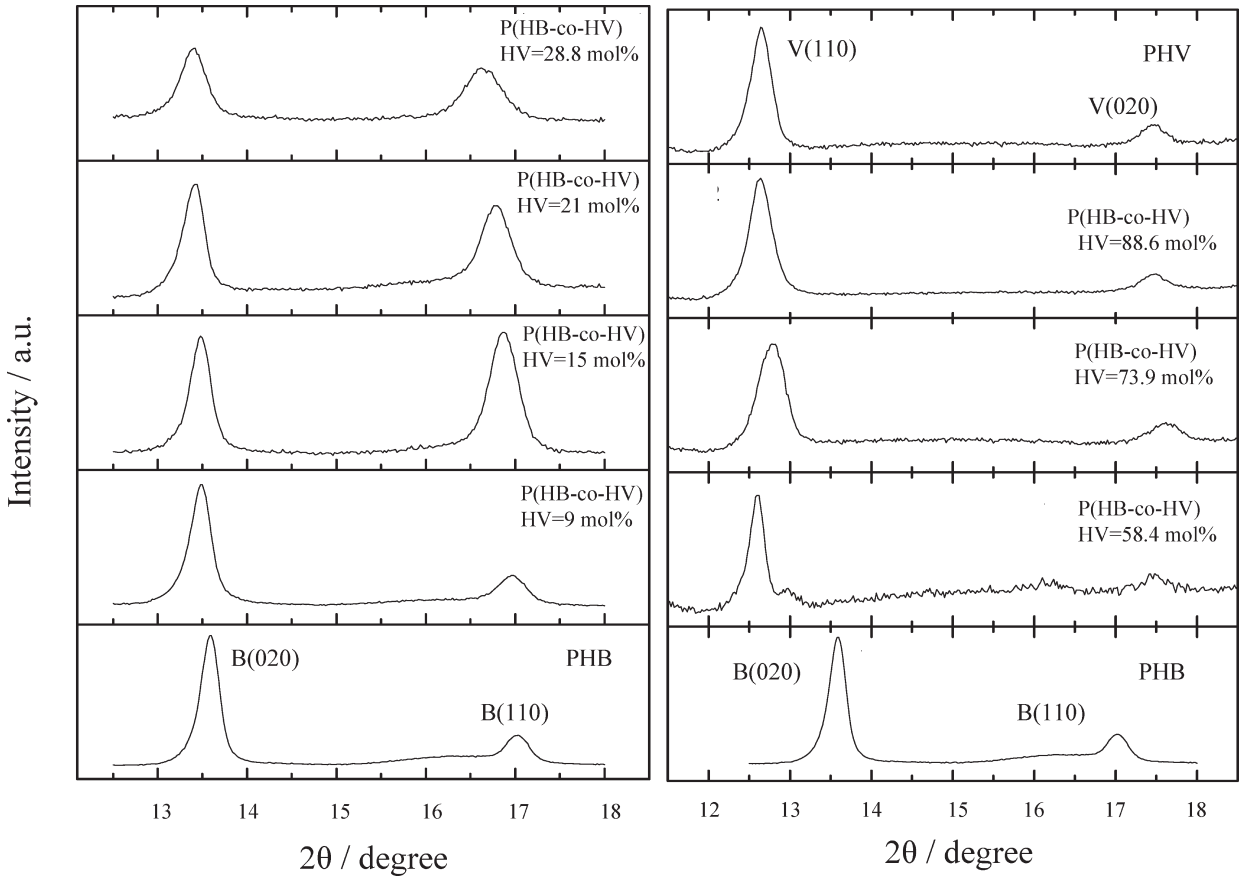

Figure 10. X-ray diffraction profiles of (a) PHB and P(HB-*co*-HV) (HV = 9, 15, 21, and 28.8 mol %) and (b) PHV, P(HB-*co*-HV) (HV = 58.4, 73.9, and 88.6 mol %), and PHB at room temperature.

dx.doi.org/10.1021/ma102723n |*Macromolecules* 2011, 44, 2829–2837

Table 2. Lattice Parameters *a* and *b* for PHB and P(HB-*co*-HV) (HV = 9, 15, 21, and 28.8 mol %)

		a/Å	*b*/Å
PHB		5.69	13.05
P(HB-*co*-HV)	HV = 9 mol %	5.70	13.15
	HV = 15 mol %	5.74	13.15
	HV = 21 mol %	5.77	13.22
	HV = 28.8 mol %	5.82	13.23

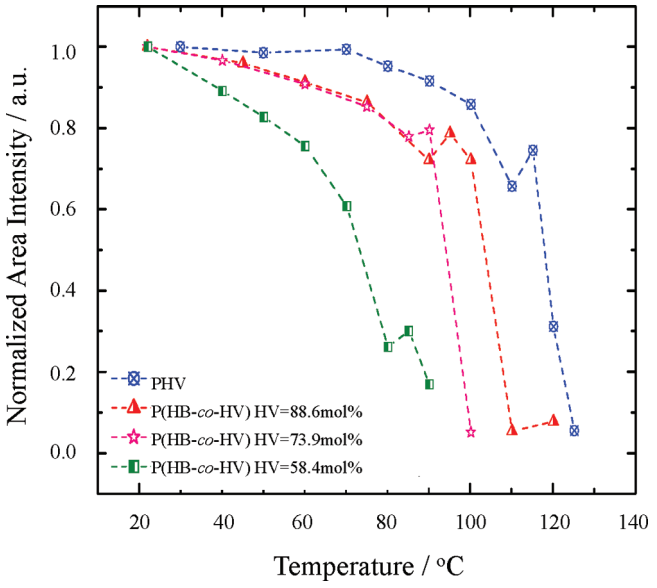

Figure 11. Plots of the normalized area intensity of (020) diffraction peak of PHV and P(HB-*co*-HV) (HV = 58.4, 73.9, and 88.6 mol %) versus temperature.

copolymers, having an isomorphic crystal structure, retain this structure up to their melting temperature.

Figure 11 shows the temperature dependence of the normalized area intensity of the (110) diffraction peaks of P(HB-*co*-HV) (HV = 58.4, 73.9, and 88.6 mol %) and PHV. The temperature dependence of P(HB-*co*-HV) (HV = 58.4, 73.9, and 88.6 mol %) is different from that of PHV. P(HB-*co*-HV) (HV = 9 and 21 mol %) shows thermal behavior similar to that of PHB, both retaining high crystallinity until just below the melting temperature. Contrarily, P(HB-*co*-HV) (HV = 58.4, 73.9, and 88.6 mol %) gradually melts, even from low temperature (significantly lower than the melting temperature). This is because both PHB and PHV are crystalline polymers and P(HB-*co*-HV) shows an isomorphic crystal structure, but HV-rich copolymers have a number of side chains that are longer than those in PHB. Therefore, the lamella structure deforms with increasing temperature, beginning at low temperatures.

The estimated values of the lattice parameters *a* and *b* of PHV and P(HB-*co*-HV) (HV = 58.4, 73.9, and 88.6 mol %) copolymers are summarized in Table 3. All of these P(HB-*co*-HV) (HV = 73.9 and 88.6 mol %) copolymers have a PHV-type crystal structure. The *a* lattice parameter of P(HB-*co*-HV) (HV = 88.6 mol %) is almost the same as that of PHV, while the *a* lattice parameter gradually increases in the P(HB-*co*-HV) (HV = 9, 15, 21, and 28.8 mol %) copolymers (Table 2). It seems that

Table 3. Lattice Parameters *a* and *b* for PHV and P(HB-*co*-HV) (HV = 58.4, 73.9, and 88.6 mol %)

		a/Å	*b*/Å
PHV		9.67	10.16
P(HB-*co*-HV)	HV = 58.4 mol %	9.96	10.30
	HV = 73.9 mol %	9.56	10.08
	HV = 88.6 mol %	9.67	10.16

the HB unit does not affect the PHV-type crystal structure because it has a CH_3 side chain that is smaller than the side chain in PHV (C_2H_5). However, the *a* lattice parameter of P(HB-*co*-HV) (HV = 58.4 mol %) copolymer shows large expansion compared to other HV-rich P(HB-*co*-HV) copolymers. The crystal structure of P(HB-*co*-HV) (HV = 58.4 mol %) copolymer shows high sensitivity to crystallization conditions because both the HB and HV units are in the same crystal structure. Therefore, P(HB-*co*-HV) (HV = 58.4 mol %) copolymer has a number of disordered structures in the lamellae.

CONCLUSION

We have investigated the crystal structure and weak intermolecular interaction of P(HB-*co*-HV) copolymers. We found that P(HB-*co*-HV) (HV = 9, 15, 21, and 28.8 mol %) copolymers have a CH···O═C hydrogen bond between the CH_3 group and the C═O group only in the HB part of their crystal structure. The strength of the hydrogen bond of P(HB-*co*-HV) (HV = 9, 15, and 21 mol %) is almost the same as that of PHB. On the other hand, HV-rich copolymers exhibit CH···O═C hydrogen bonding between the CH_2 group and the C═O group, and its strength becomes less than that of PHV with a decrease in HV content. This is due to the difference in the length of the side chain between HB and HV units. Moreover, P(HB-*co*-HV) (HV = 58.4 mol %) has very weak C−H···O═C hydrogen bonds because P(HB-*co*-HV) copolymer with an HV content of around 50 mol % shows a transition in its crystal structure from the PHB-type to the PHV-type. The crystal structure of P(HB-*co*-HV) (HV = 58.4 mol %) collapses more easily than those of PHB, PHV, and other P(HB-*co*-HV) copolymers (HV = 9, 15, 21, 22.8, 73.9, and 88.6 mol %). In fact, the temperature-dependent IR spectra and WAXD profiles of P(HB-*co*-HV) (HV = 58.4 mol %) show that the crystal structure collapses even at low temperatures, as P(HB-*co*-HV) (HV = 58.4 mol %) exhibits little hydrogen bonding either of the CH_3···O═C type or of the CH_2···O═C type. Thus, it is very likely that the two types of CH···O═C hydrogen bonding (CH_3···O═C and CH_2···O═C) stabilize the crystal structures of PHB, PHV, and P(HB-*co*-HV) copolymers. Even if the CH···O═C hydrogen bonding is relatively weak, it is extremely important for the stabilization of lamellae.

ASSOCIATED CONTENT

Supporting Information. Experimental details. This material is available free of charge via the Internet at http://pubs.acs.org.

AUTHOR INFORMATION

Corresponding Author
*E-mail: hsato@kwansei.ac.jp.

■ ACKNOWLEDGMENT

This work was supported by Kwansei-Gakuin University "Special Research" project, 2004−2014, Grant-in-Aid for Scientific Research (C) from MEXT (No. 20550197), Grant-in-Aid for Scientific Research (C) from MEXT (No. 20550026), and Shiseido Female Researcher Science Grant (2009−2010).

■ REFERENCES

(1) Lemoigne, M. *Bull. Soc. Chim. Biol.* **1926**, *8*, 770.
(2) Doi, Y. *Microbial Polyesters*; VCH Publishers: New York, 1990.
(3) Vert, M. *Biomacromolecules* **2005**, *6*, 538.
(4) Chiellini, E.; Solaro, R. *Recent Advances in Biodegradable Polymers and Plastics*; Wiley-VCH: Weinheim, 2003.
(5) Doi, Y. *ICBP 2003 First IUPAC International Conference on Bio-Based Polymers, Macromolecular Bioscience*; Wiley-VCH: Weinheim, 2004; Vol.4, Issue 3.
(6) Bastioli, C. *Handbook of Biodegradable Polymers*; Rapra Technology Limited: 2005.
(7) Satkowski, M. M.; Melik, D. H.; Autran, J.-P.; Green, P. R.; Noda, I.; Schechtman, L. A. In *Biopolymers*; Steinbüchel, A., Doi, Y., Eds.; Wiley-VCH: Wienheim, 2001; p 231.
(8) Iwata, T.; Aoyagi, Y.; Fujita, M.; Yamane, H.; Doi, Y.; Suzuki, Y.; Takeuchi, A.; Uesugi, K. *Macromol. Rapid Commun.* **2004**, *25*, 1100.
(9) Doi, Y.; Kitamura, S.; Abe, H. *Macromolecules* **1995**, *28*, 4822.
(10) Kobayashi, G.; Shiotani, T.; Shima, Y.; Doi, Y. In *Biodegradable Plastics and Polymers*; Doi, Y., Fukuda, K., Eds.; Elsevier: Amsterdam, 1994; p 410.
(11) Kunioka, M.; Tamaki, A.; Doi, Y. *Macromolecules* **1989**, *22*, 694.
(12) Bloembergen, S.; Holden, D. A.; Hamer, G. K.; Bluhm, T. L.; Marchessault, R. H. *Macromolecules* **1986**, *19* (11), 2865.
(13) Doi, Y.; Kunioka, M.; Tamaki, A.; Nakamura, Y.; Soga, K. *Makromol. Chem.* **1988**, *189*, 1077–1086.
(14) Mitomo, H.; Morishita, N.; Doi, Y. *Macromolecules* **1993**, *26*, 5809–5811.
(15) Allegra, G.; Bassi, I. W. *Adv. Polym. Sci.* **1969**, *6*, 549.
(16) Bluhm, T. L.; Hamer, G. K.; Marchessult, R. H. *Macromolecules* **1986**, *19*, 2871–2876.
(17) Yamada, S.; Wang, L.; Asakawa, N.; Yoshie, N.; Inoue, Y. *Macromolecules* **2001**, *34*, 4659.
(18) Yoshie, N.; Saito, M.; Inoue, Y. *Macromolecules* **2001**, *34*, 8953–8960.
(19) Mitomo, H.; Morishita, N.; Doi, Y. *Polymer* **1995**, *36*, 2573–2578.
(20) Sato, H.; Ando, Y.; Dybal, J.; Iwata, T.; Noda, I.; Ozaki, Y. *Macromolecules* **2008**, *41*, 4305–4312.
(21) Sato, H.; Mori, K.; Murakami, R.; Ando, Y.; Takahashi, I.; Zhang, J.; Terauchi, H.; Hirose, F.; Senda, K.; Tashiro, K.; Noda, I.; Ozaki, Y. *Macromolecules* **2006**, *39*, 1525.
(22) Sato, H.; Nakamura, M.; Padermshoke, A.; Yamaguchi, H.; Terauchi, H.; Ekgasit, S.; Noda, I.; Ozaki, Y. *Macromolecules* **2004**, *37*, 3763.
(23) Sato, H.; Murakami, R.; Padermshoke, A.; Hirose, F.; Senda, K.; Noda, I.; Ozaki, Y. *Macromolecules* **2004**, *37*, 7203.
(24) Sato, H.; Dybal, J.; Murakami, R.; Noda, I.; Ozaki, Y. *J. Mol. Struct.* **2005**, *744−747*, 35.
(25) Marchessault, R. H.; Kawada, J. *Macromolecules* **2004**, *37*, 7418.
(26) Marchessault, R. H.; Yu, G. In *Biopolymers, Polyesters II*; Doi, Y., Steinbüchel, A., Eds.; Wiley-VCH: Wienheim, 2002; p 157.
(27) Iwata, T.; Doi, Y. *Macromolecules* **2000**, *33*, 5559.